

Manipulating molecular orientation in vapor-deposited organic semiconductor glasses via in-situ electric fields: a molecular dynamics study

Marta Rodríguez-López^{1,2}, Marta Gonzalez-Silveira^{1,2}, Antonio Cappai³, Riccardo Dettori³, Cristian Rodríguez-Tinoco^{1,2}, Claudio Melis³, Luciano Colombo³, Javier Rodríguez-Viejo^{1,2}

1 Department of Physics, Facultat de Ciències, Universitat Autònoma de Barcelona, 08193 Bellaterra, Barcelona, Spain

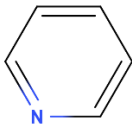
2 Catalan Institute of Nanoscience and Nanotechnology (ICN2), CSIC and BIST, Campus UAB, 08193 Bellaterra, Barcelona, Spain

3 Department of Physics, University of Cagliari, Monserrato, Cagliari, 09042 Italy

Supplementary Information

A- Electric dipole moment of heterocyclic molecules for method validation

Density Functional Theory using the Gaussian package was employed to calculate the electric dipole moment of TPD, TPD-Br1 and TPD-Br2. Five reference molecules have been chosen for proving the level of accuracy of the calculations for determining the electric dipole moment of TPD, TPD-Br1 and TPD-Br2. Table A.1. exhibits the comparison between the calculated DFT dipoles (μ_{DFT}) and the experimental values (μ_{exp}). Our calculations, with an overall RMSD error of 0.09D, are in great accordance with the values reported in the literature [a-d].

Molecule	Structure	$\mu_{DFT} \pm 0.09$ (D)	μ_{exp} (D)
Pyridine		2.209	2.190 [a]

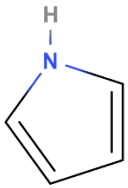
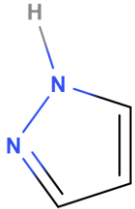
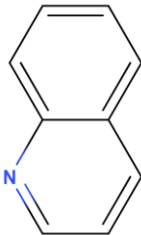
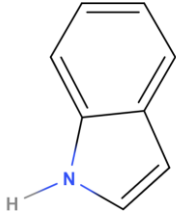
Pyrrole		1.937	1.840 [a]
Pyrazole		2.292	2.214 [b]
Quinoline		2.05	2.18 [c]
Indole		2.16	2.05 [d]

Table A.1. Benchmark calculations to assess the accuracy of the present computational setup. Gas phase electric dipole moment in Debye for the five reference molecules used to assess the method validity. μ_{exp} refer to electric dipole moment experimental values [a-d]. Uncertainties on our values are taken as the RSM deviation of the sample.

B- Deposition velocity calculation

Molecules being evaporated by PVD in the molecular dynamics simulations in this work contain a certain velocity towards the substrate that ensures a great ratio of molecules landing in the substrate. That velocity is taken as the mean velocity \bar{c} given by the kinetic theory of glasses, given by:

$$\bar{c} = \frac{4F}{n} \quad (\text{b.1})$$

where n is the number of molecules per unit volume and F is the flux of molecules over a surface. On one hand, the flux is simply determined by the product of the density of the molecule ρ times the evaporation rate R :

$$F = \rho \cdot R \quad (\text{b.2})$$

On the other hand, the number of molecules per unit volume will be extracted from the ideal gas equation:

$$n = \frac{p}{K_B T} \quad (\text{b.3})$$

where p is the pressure of the evaporation chamber, K_B the Boltzmann constant and T the fusion temperature at which the molecules evaporate. The values involved in the calculations are derived from experimental parameters for the preparation of TPD vapor-deposited glasses or from literature, and are shown in Table B.1. As a result, the scalar velocity of the molecules during the evaporation, calculated from Eq.(c.1) results in $\bar{c} = 30.76 \text{ m/s}$.

ρ^*	$1.08 \text{ g/cm}^2 = 1.26 \cdot 10^{27} \text{ moles/m}^3$
R	0.1 nm/s
F	$1.26 \cdot 10^{17} \text{ moles/m}^2\text{s}$
p	$10^{-7} \text{ mbar} = 10^{-5} \text{ Pa}$
T	$\sim 170 \text{ }^\circ\text{C} = 443 \text{ K}$
K_B	$1.38 \cdot 10^{-23} \text{ J}$
n	$1.64 \cdot 10^{16} \text{ moles/m}^3$

Table B.1. Parameters needed for calculating the mean velocity of TPD molecules during evaporation, extracted both from literature and from experimental conditions. *Density of TPD is extracted from Sigma Aldrich product specifications. Rate R , pressure p and temperature T values are extracted from experimental values.

C- Halogenation of TPD

In this work, halogenated versions of the starting molecules were generated by addition of bromine (Br), chlorine (Cl) and fluorine (F) in order to check the effect of halogenation upon permanent electric dipole moment. The sites of substitution, hereafter labeled as R, are clearly depicted in Fig.C.1. In the case of pristine molecule, R correspond to H atoms, while in the case of halogenation, in all the R-sites of the molecule the corresponding halogen was substituted.

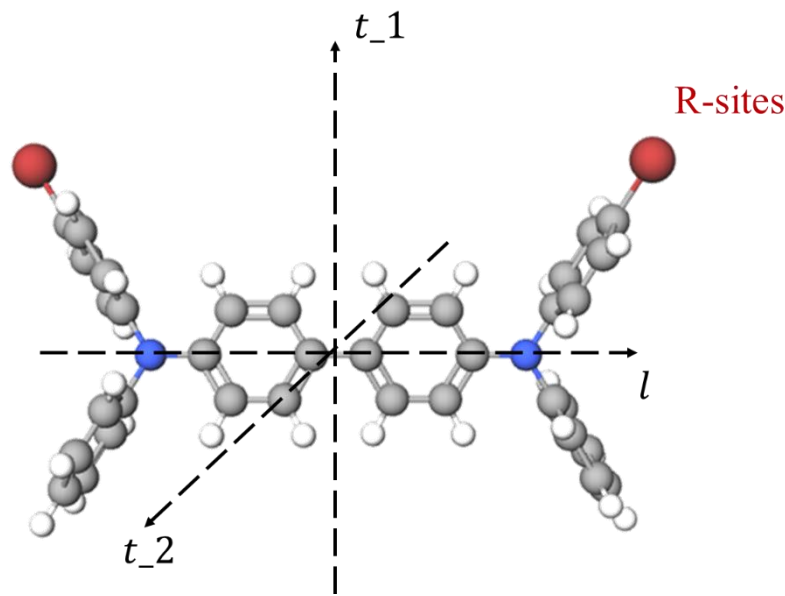


Figure C.1. Chemical structure of N,N'-Bis(3-methylphenyl)-N,N'-diphenylbenzidine (TPD) without methyl groups, with R indicating the halogenation sites (assuming R as hydrogen in pristine molecule).

The gas phase electric dipole moment for the molecules of interest before and after halogenation are listed in Table C.1: as expected, a remarkable increase is observed in all molecules after halogenation. Bromine appears to be the best candidate, giving rise to an increase of $\sim 145\%$ in the y component in the case of TPD.

R-site substituent	μ_l (D)	μ_{t_1} (D)	μ_{t_2} (D)	μ (D)
H (Pristine molecule)	-0.31	0.26	0.04	0.41
Br	-0.06	4.05	0.12	4.05
Cl	-0.08	3.97	0.12	3.97
F	-0.08	2.49	0.27	2.50

Table C.1. Gas phase cartesian components of the electric dipole moment $\vec{\mu}$ (in Debye) for TPD before (pristine) and after halogenation with substituents H, Br1, Cl and F. Reference axis are represented in Fig.B.1

D-Vector diagrams and electric dipole moment components histograms for TPD-Br1 under 10^5 V/m and 10^7 V/m at $T_f=300$ K

The distribution of the molecular permanent electric dipole moment of vapor deposited TPD-Br1 glasses under electric fields of 10^5 V/m and 10^7 V/m is presented in Fig.D.1. These electric fields do not induce any change in the molecular orientation of the glass, as the vectorial distribution remains identical to glasses deposited without the influence of an electric field, and no preferential orientation of the electric dipole moment is observed.

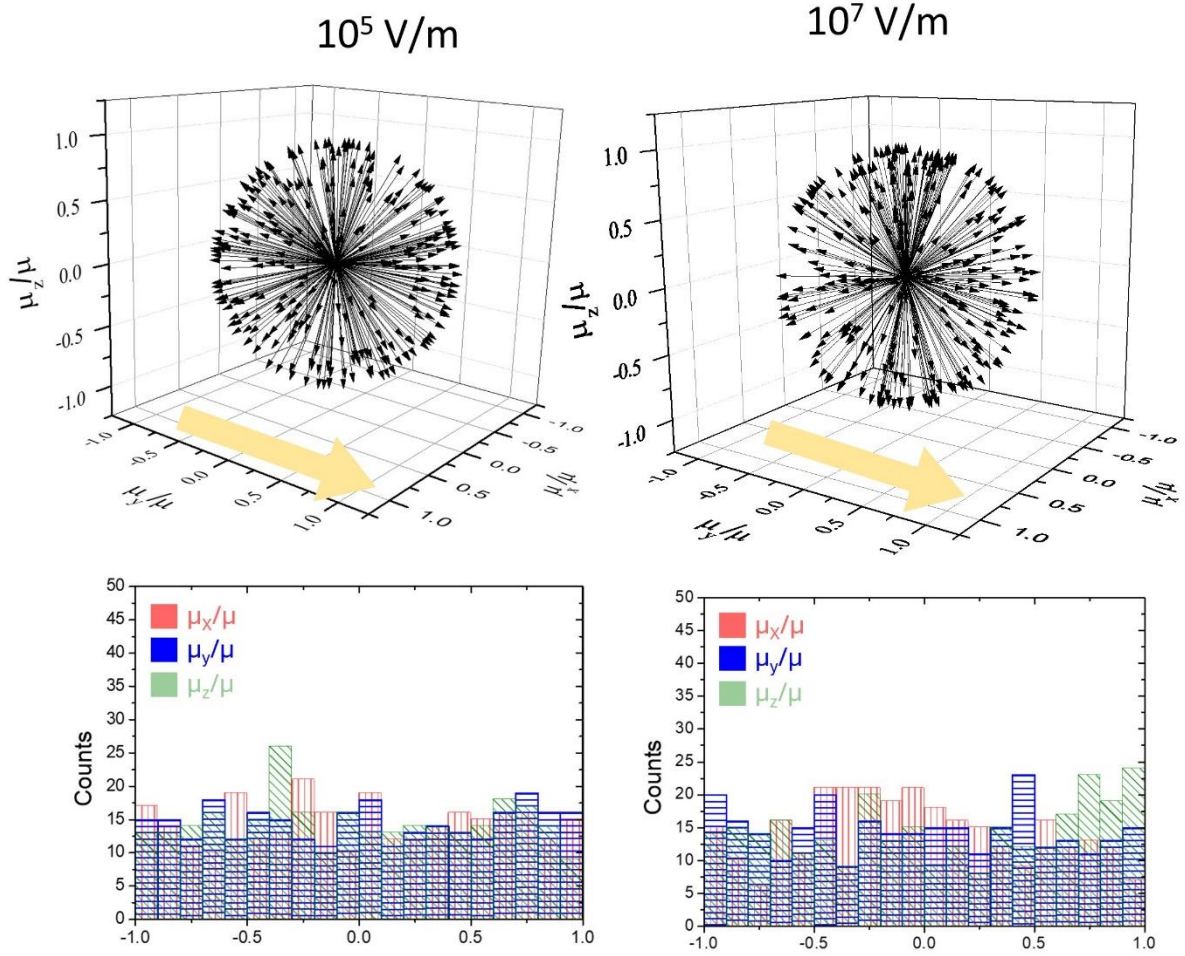
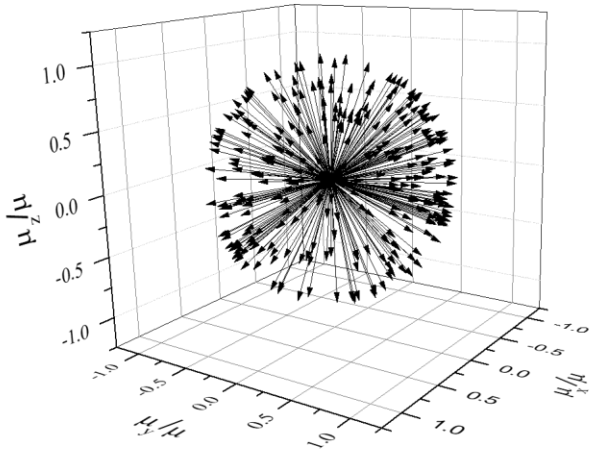


Figure D.1. Representation of the electric dipole moment coordinates weighted by the modulus of the electric dipole moment of the 300 molecules in the MD vapor deposited glasses for TPD-Br1 prepared at 300K and under 10^5 and 10^7 electric fields along \hat{y} (direction of the field in yellow). The histograms with the counts of the μ_x/μ (in orange, vertical lines) μ_y/μ (in blue, horizontal lines) and μ_z/μ (in green, diagonal lines) of each specific case are also presented.

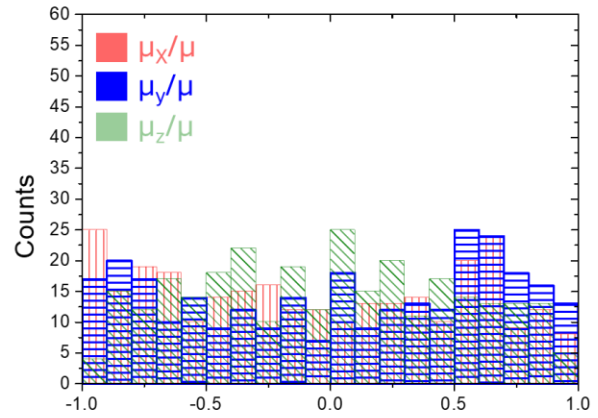
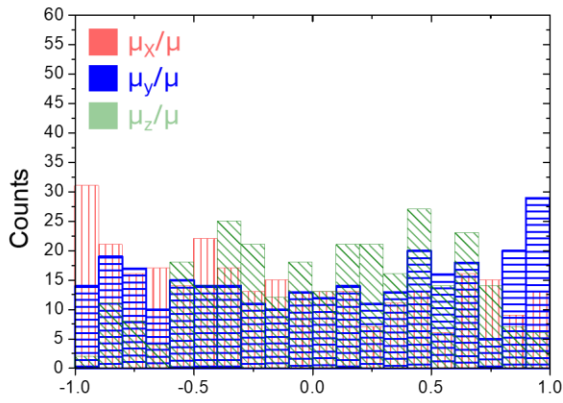
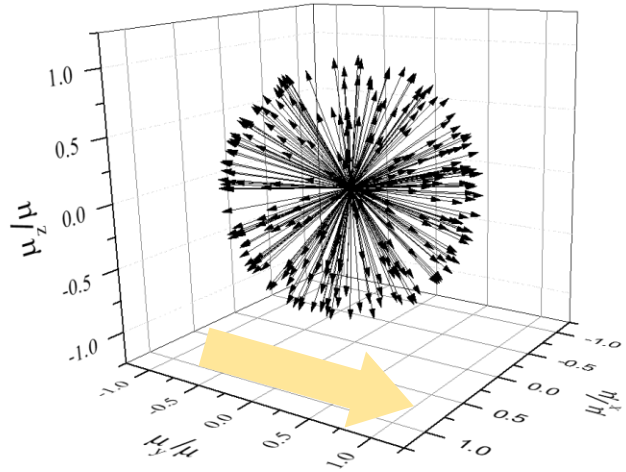
E-Vector diagrams and electric dipole moment components histograms for TPD-Br2 under 0, 10^5 V/m and 10^7 V/m and 10^9 V/m at $T_f=300$ K

The distribution of the molecular permanent electric dipole moment of vapor deposited TPD-Br2 glasses under electric fields of 0, 10^5 , 10^7 and 10^9 V/m (in plane and out of plane) is presented in Fig.E.1. As well as for the case of TPD-Br1, electric fields below 10^9 V/m are unable to tune the orientation of the molecules in a TPD-Br2 glass prepared at 300K, as shown in Fig(D.1).

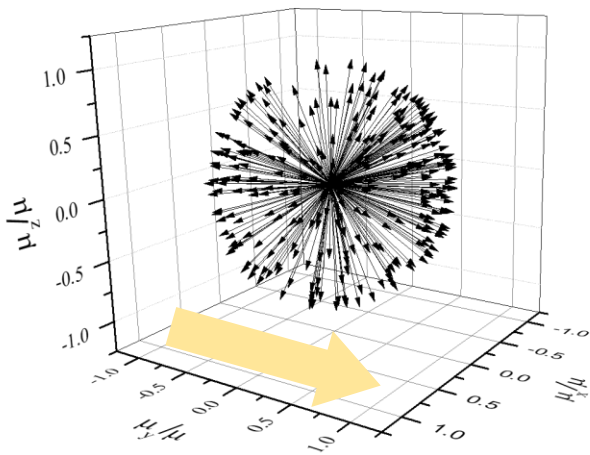
0 V/m



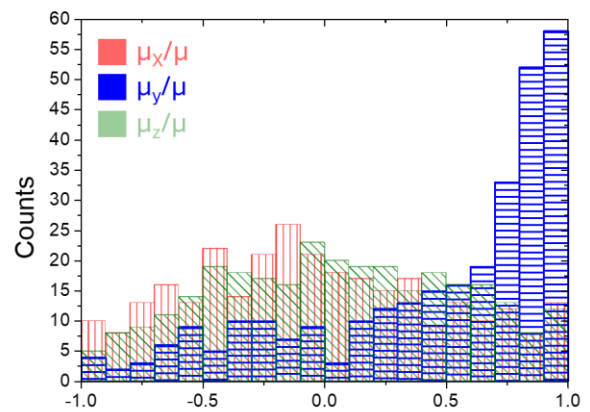
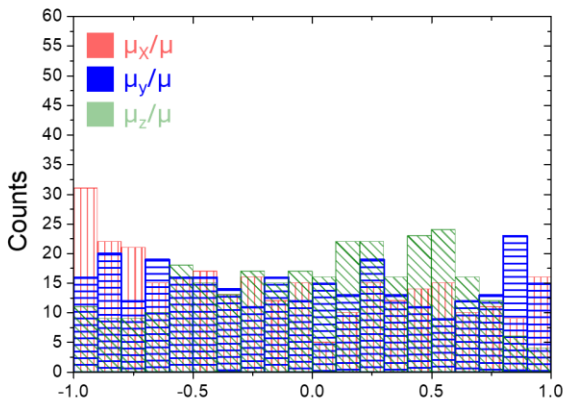
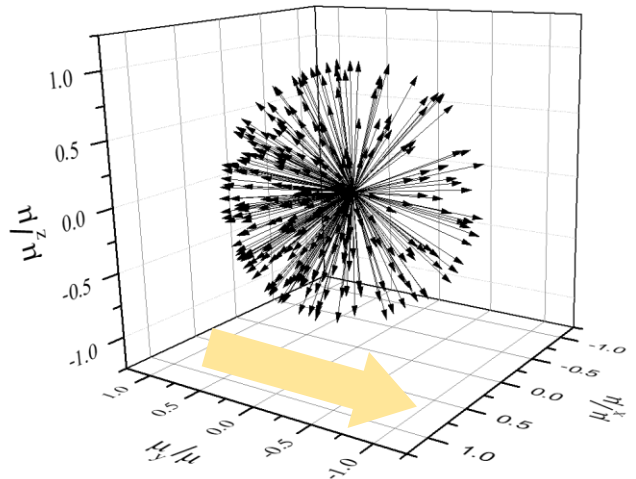
10^5 V/m



10^7 V/m



10^9 V/m



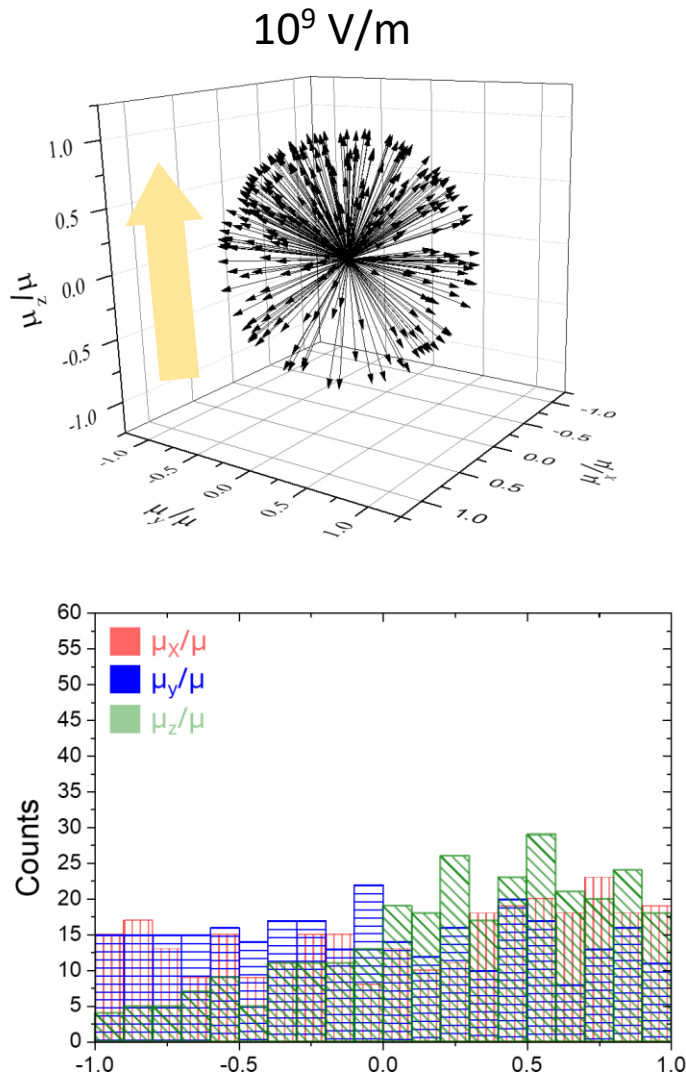


Figure E.1. Representation of the electric dipole moments of a 300 molecules vapor deposited TPD-Br2 glass, prepared at 300K under electric fields in y with intensities of 0 V/m, 10^5 V/m, 10^7 V/m, 10^9 V/m.

F- Computational procedure used to estimate the TPD glass transition temperature.

The TPD molecule was initially relaxed with a geometry optimization. Quenched-from-the-melt (QFTM) samples were realized by starting with supercell of 343 molecules, obtained by replicating the starting molecule 7 times in each direction. A box relaxation with energy minimization then followed. The quench-from-the melt procedure required a first annealing of the sample, which was heated up to 1200K and equilibrated at that temperature for 300 ps, to fully melt and randomize molecular positions. Then a first cooling at a fixed cooling rate of 2×10^{-4} K/fs was performed to cooldown the sample at a temperature of 540K and a further equilibration of 100 ps then followed. At this stage

the sample is still liquid (from experimental measurements it is known that TPD glass transition temperature is $T_{\text{exp}}^g = 333\text{K}$ [e]) and we considered this as the starting state point for the QFTM protocol. We then cooled our sample, using the NVT ensemble, with five different cooling rates, namely $\gamma_{\text{cool}} = 10^{-1}, 10^{-2}, 10^{-3}, 10^{-4},$ and 10^{-5} K/fs saving a configuration each 10K. Such configuration was kept at its reference temperature for further 200 ps with a constant pressure run in order to reach the equilibrium density. Obtained densities for $\gamma_{\text{cool}} = 10^{-5}$ are slightly lower than experimental densities [f], which for conventional TPD systems are found to be around 1.08 g/cm³. However, such discrepancy can be ascribable to the adopted force-field since previous simulated TPD sample obtained with a different interatomic potential showed higher densities, in better agreement with the experiments [g]. It is worth noting that a change in the slope of the $\rho(T)$ trend can be observed between 300 and 350K: as we will point out later in the text, such temperature is related to the glass transition.

A crucial quantity when dealing with glasses is the inherent structure energy EIS[h], which is the potential energy of the minimum in the energy landscape associated with those thermodynamic conditions. To calculate EIS, we considered the configurations saved during the cooling phase illustrated in the previous section: once they reached their equilibrium density, they were simulated for further 100 ps in the NVT ensemble. During this equilibration, a configuration was saved each 500 fs, to have statistically independent frames. Such configurations were fully minimized according to the FIRE algorithm obtaining a set of energies relative to the local minima of the considered configuration. Finally, the inherent structure energy was obtained by averaging a subset of such energies. The results are shown in Fig F.1a. While the films obtained with the faster cooling rate do not show interesting features and a temperature independent EIS, for $\gamma_{\text{cool}} = 10^{-4}$, and especially 10^{-5} a non-Arrhenius behavior is obtained. In fact, as shown in Fig. F.1b, where we plot the derivative of EIS with respect to temperature, a sharp discontinuity corresponding to a slope change is observed at $T = 330\text{K}$. In particular, at higher temperatures (not shown in this work) the system is fully ergodic, it behaves as a liquid, and it has sufficient kinetic energy to explore the energy landscape. During the cooling process, the system undergoes a super-cooled phase in which its dynamics is landscape-influenced because the stable configurations sampled by the molecules are strongly influenced by the temperature. Below the glass transition temperature T_g , the system is frozen in a particular configuration because the energy barrier separating adjacent minima

cannot be overcome with its current kinetic energy. We found that the value of T_g shows a satisfactory agreement with the experimental results [e].

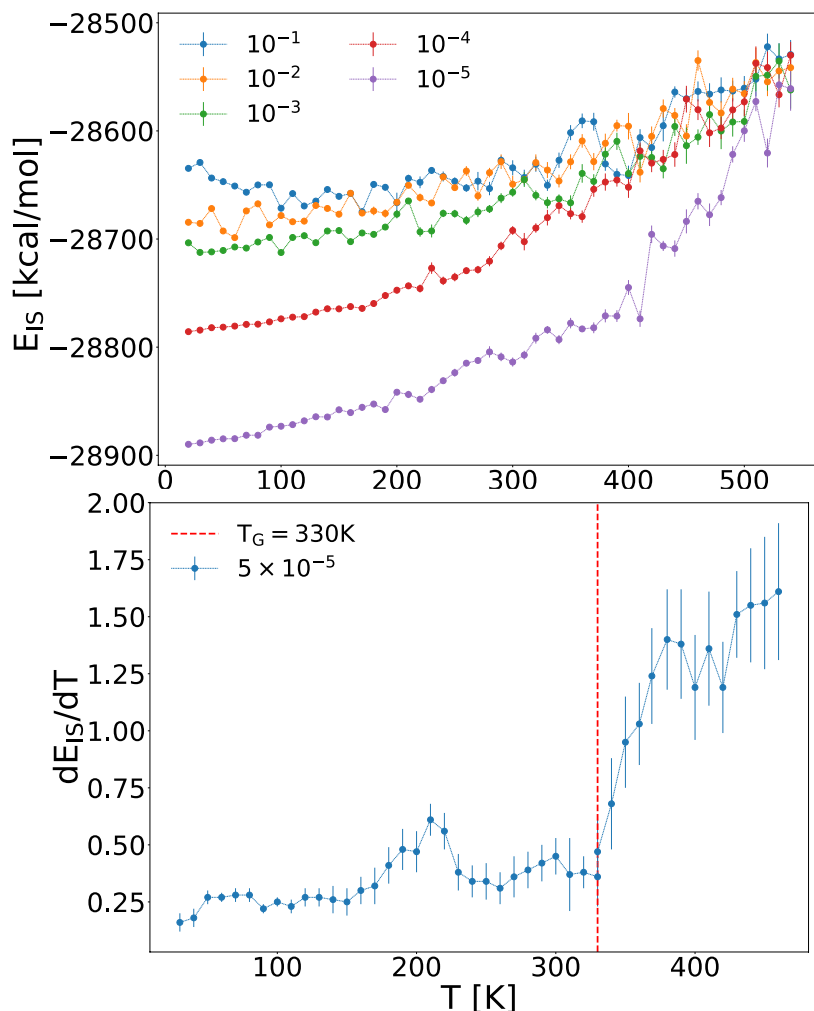


Figure F.1. top: Inherent structure energies calculated for the freestanding QFTM film of TPD, with five different cooling rate. bottom: Temperature derivative of EIS as a function of temperature.

G- Computational approach for estimating ionization potentials and molecular polarizability.

To calculate the polarizability of the TPD molecule and its halogenated derivatives, we applied the same computational protocol used for determining the Cartesian components of the dipole moment. Specifically, the calculations were performed using the same combination of functional and Gaussian basis set, which are key parameters influencing the accuracy of the results.

For the determination of polarizability, we used the implementation available in Gaussian16. This method applies a small external electric field to compute the induced dipole moments, allowing the polarizability tensor to be determined. The perturbative approach is based on calculating the induced dipole moment, with the polarizability tensor α being derived from the linear relationship:

$$\mu = \mu_0 + \alpha E$$

where

- μ is the dipole moment under the applied field,
- μ_0 is the dipole moment in the absence of the field, and
- E is the applied electric field.

Gaussian16, by default applies an electric field of 0.001 atomic units (a.u.), equivalent to 5×10^7 V/m, which allows accurate calculations of polarizabilities through perturbative methods. No significant changes were observed when the field strength was increased by an order of magnitude (up to 0.01 a.u.). The field is applied along three orthogonal axes (x, y, z), allowing for the calculation of all six independent components of the polarizability tensor.

The same computational setup was used to calculate the ionization potential (IP), approximated as the negative of the highest occupied molecular orbital (HOMO) energy. Electronic eigenvalues for all molecular orbitals were computed to obtain these values. To estimate the threshold for possible potential field ionization of the molecules, the ionization potential was divided by a typical TPD molecular size. With the estimated DFT ionization potential around 7 eV and an approximate molecular size of 1 nm, the corresponding electric field is estimated to be 7×10^9 V/m. As the fields applied in our MD simulations were significantly weaker, field-ionization phenomena are not expected to occur in the simulations. The experimental HOMO for the TPD molecule is around 5.5 eV, which, reproducing the same calculation as for the DFT one, yields ionization fields of around $5.5 \cdot 10^9$ V/m, which would still be higher than the applied fields in our simulations.

References

- [a] R. D. Nelson Jr, D. R. Lide Jr, and A. A. Maryott, *Selected values of electric dipole moments for molecules in the gas phase*, Tech. Rep. (National Standard Reference Data System, 1967).
- [b] W. H. Kirchhoff, *The microwave spectrum and dipole moment of pyrazole*, Journal of the American Chemical Society 89, 1312 (1967). <https://doi.org/10.1021/ja00982a006>
- [c] Alan Hinchliffe, Humberto J. Soscún Machado, *Ab initio studies of the dipole polarizabilities of conjugated molecules: Part 3. One electron properties, dipole polarizability and first hyperpolarizability of quinoline and isoquinoline*, Journal of Molecular Structure: THEOCHEM, Volume 312, Issue 1, 1994, Pages 57-67, [https://doi.org/10.1016/S0166-1280\(09\)80007-9](https://doi.org/10.1016/S0166-1280(09)80007-9).
- [d] A. Katritzky, Physical methods in heterocyclic chemistry, Vol. 3 (Elsevier, 2012).
- [e] Joan Ràfols-Ribé, Riccardo Dettori, Pablo Ferrando-Villalba, Marta Gonzalez-Silveira, Llibertat Abad, Aitor F. Lopeandía, Luciano Colombo, and Javier Rodríguez-Viejo, Evidence of thermal transport anisotropy in stable glasses of vapor deposited organic molecules. Physical Review Materials 2, 035603 (2018).
- [f] D. M. Walters, R. Richert, and M. D. Ediger, The Journal of Chemical Physics 142, 134504 (2015).
- [g] R. Dettori and L. Colombo, Istituto Lombardo – Accademia di Scienze e Lettere - Incontri di Studio. (lug. 2018) (2018), 10.4081/incontri.2018.378.
- [h] F. H. Stillinger and T. A. Weber, Science 225, 983 (1984),